Available online at www.sciencedirect.com
ScienceDirect
Surface & Coatings Technology 201 (2007) 8230–8236
SURFACE & COATINGS TECHNOLOGY
www.elsevier.com/locate/surfcoat

Radiation induced modifications in ultra-high molecular weight polyethylene

C.P. Stephens [a], R.S. Benson [a,*], M. Chipara [b]

[a] Department of Materials Science and Engineering, The University of Tennessee, Knoxville, TN 37996-2200, United States
[b] Department of Physics and Geology, University of Texas-Pan American, Edinburg, TX 78541, United States

Available online 16 March 2007

Abstract

The effect of proton irradiation dose on the morphology of ultra high molecular weight polyethylene (UHMWPE) was studied. The radiation dose was varied from 0.09402 to 0.87 Mrads. The thermal behavior of the irradiated samples was investigated by submission to two heating cycles. The proton irradiation produces morphological changes in the mole fraction of crystallizable units, sequence length distribution, and crystallite thickness and distribution. The type of morphological changes is dependent on irradiation dose and thermal cycle. The low proton radiation dose produces only slight changes in the morphology of UHMWPE. More pronounced morphological changes are observed for the higher proton radiation dose.

Keywords: Proton; Radiation; Polyethylene; Sequence; Length; Crystallinity

1. Introduction

The radiation in the environment of space consists of accelerated electrons, protons, and heavy ions. Protons dominate the spectrum of accelerated particles in galactic cosmic rays, solar flares, and the inner Van Allen belt. The energy deposited by protons along their incident trajectory produces chemical and physical modifications in target materials. In the case of polymers, biopolymers, and even humans, the energy deposited by incident protons triggers the formation of free radicals leading to alternative reaction pathways. To protect astronauts and sensitive devices during space missions, it is necessary to use materials capable of absorbing or degrading the energy of impinging particles without undergoing significant changes in their chemical or physical properties. Polyethylene has great potential as a shielding material for space application due to its high hydrogen content, simple elemental composition, and a nucleus not susceptible to release neutrons through nuclear reaction. In addition, the availability of higher molecular mass polyethylene, i.e., ultra high molecular weight polyethylene (UHMWPE), could lead to further enhancement of shielding and structural properties.

The interaction between polymers and ionizing radiation leads to electronic excitation, phonons, ionization, ion pair formation, radical formation, and chain scission [1–11]. If the segmental motions of the macromolecular chains are sufficiently high, the free radicals recombine. This process may increase the length of the chain, add long side branches, and finally may crosslink the irradiated polymer. Basically, the irradiation of polymers involves two competing processes: chain scission (termination in disproportionation) and cross-linking (termination in intermolecular cross-links). Thermodynamic factors and in particular the jump frequency of segments controls the dominant degradation process of polymers subjected to irradiation. Both scissions and cross-linking processes affect the mechanical properties of the pristine polymer (such as hardness, wear, elongation at break, tensile strength at yield, and Young modulus). In most cases, the ionizing radiation triggers both scission and cross-linking reactions. The balance between these reactions characterizes the overall response of the polymer to ionizing radiation. The presence of oxygen shifts this equilibrium towards scission reactions; accordingly a polymer that undergoes dominant crosslinking reactions when subjected to ionizing radiation in vacuum may exhibit dominant scission reactions if irradiated in air. As a consequence, the presence of molecular oxygen during irradiation leads to a higher degree of chain scission and

* Corresponding author.
E-mail address: rbenson1@utk.edu (R.S. Benson).

0257-8972/$ - see front matter © 2007 Published by Elsevier B.V.
doi:10.1016/j.surfcoat.2006.03.055

Table 1
Irradiation doses and incidence energy

Sample description	Energy of incidence (MeV)	Absorbed dose (Mrads)	L_{el} (MeV cm^2/mg)	L_{nucl} (MeV cm^2/mg)	L_{tot} (MeV cm^2/mg)
Control (4 samples)	0	0	0	0	0
Low dose (8 samples)	198	0.094	0.00482	1.83e-6	0.00482
	186	0.096	0.00502	1.943e-6	0.00502
	160	0.103	0.00556	2.23e-6	0.00556
	120	0.123	0.00681	2.91e-6	0.00681
	27	0.37	0.02203	1.730e-5	0.02203
High dose (3 samples)	195	0.68	0.00487	1.86e-6	0.00487
	127	0.83	0.00654	2.76e-6	0.00654
	133	0.87	0.00633	2.65-6	0.00633

deterioration of mechanical properties. In an inert environment, intermolecular cross-linking is the predominant process during ionizing irradiation of polyethylene at room temperature. Recent work from our laboratory showed that improvement in the mechanical properties of the gamma-irradiated polyethylene can be ascribed to changes in the morphology [3]. In the present work the radiation component of the space environment is simulated by proton beams accelerated up to 200 MeV. Differential scanning calorimetry (DSC) is used to study the morphological changes in UHMWPE induced by high and low doses of proton irradiation.

2. Experimental

2.1. Proton irradiation procedures

All UHMWPE samples (Tivar 1000 produced by Poly Hi Solidur) were machined into discs with a radius of 1.75-inch and thickness of 0.25-inch. The samples were irradiated with protons at a fluence of 3.6×10^{17} protons/m^2 and a flux of 2×10^{14} protons/m^{2}s (low dose irradiation) and a fluence of about 2×10^{18} protons/m^2 (flux of about 3×10^{14} protons/m^{2}s) for the high dose irradiation. All irradiations were carried out in air, at room temperature. The incident energy and total dose for each sample is listed in Table 1. The Linear Energy Transfer (LET) was estimated by using the standard SRIM program, with a corrected density of 0.97 g/cm^3 for UHMWPE. The LET was estimated for incident and emergent faces of the sample and averaged. Both electronic and nuclear contributions were added. The energy deposited by the beam in each sample was calculated by multiplying the average LET by the thickness of the sample. PMMA spacers of different thickness were used between UHMWPE samples. The samples were stacked together for irradiation, see Fig. 1. The sample holder was made of a PVC (Polyvinylchloride) tube. The spacer introduced a layer of air with a thickness of about 5 mm between samples (in order to decrease heat accumulation during the irradiation). The energy deposited by the incident particle in the target is dominated by the electronic component, which is larger by

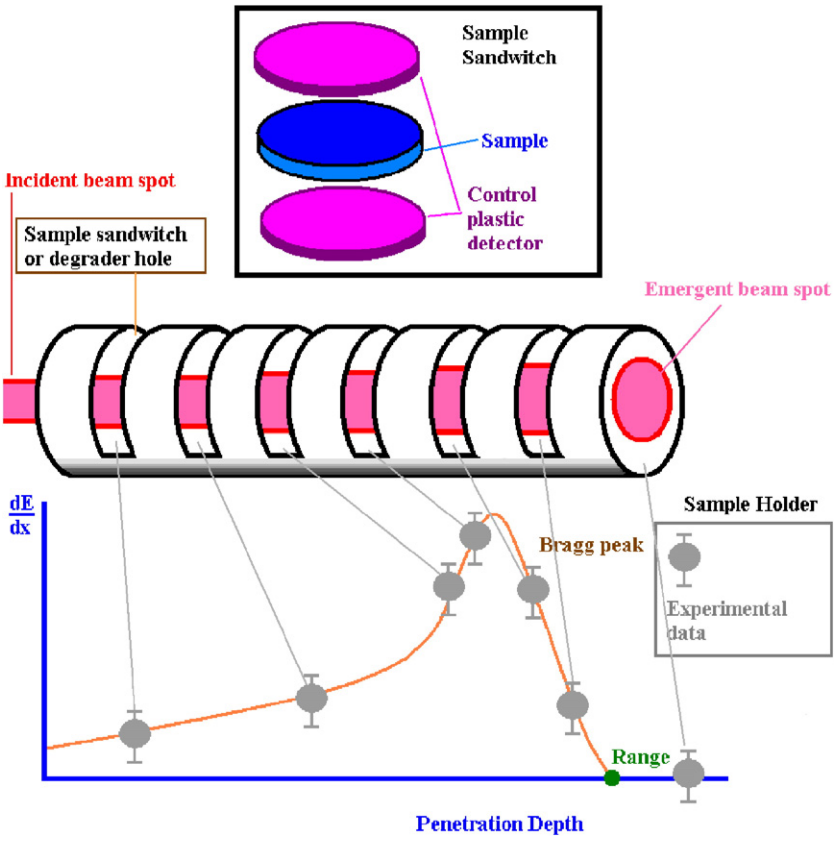

Fig. 1.

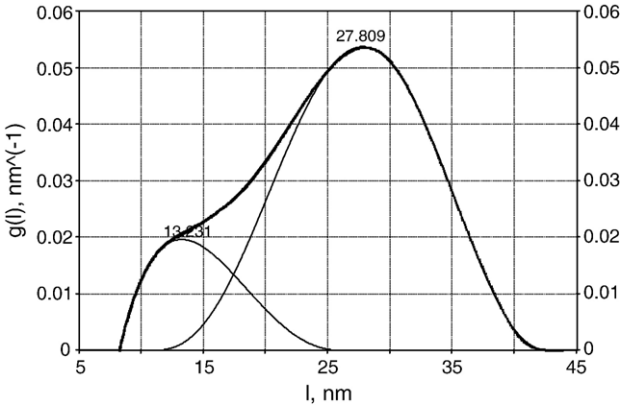

Fig. 2.

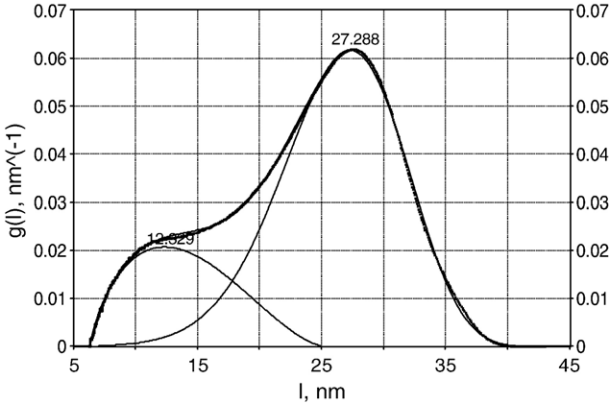

Fig. 4. Deconvolution of $g(l)$ distribution for UHMWPE Sample exposed to high radiation dose.

about 2 orders of magnitude than the nuclear stopping power. The sample holder had about 40 positions for samples and it was calculated to allow for a total "sample length" longer by about 50% that the range of 200 MeV protons in polyethylene.

2.2. Differential Scanning Calorimetry (DSC)

A 1-mm thick disc heated from 75 °C to 180 °C at 1 °C min^{-1}, cooled from 180 °C to 75 °C at 1 °C min^{-1} and then reheated (heat treated) from 75 °C to 180 °C at 1 °C min^{-1}. Data collection was conducted at a slow rate to avoid artificial increase of the melting temperature, T_m, to and above the theoretical T_m^o value due to the high degree of chain entanglement and cross-linking found in these irradiated UHMWPE samples [12]. The Mettler Toledo 821e DSC is calibrated using an Indium and Zinc standard. The degree of crystallinity, X_c, is determined from Eq. (1).

$$X_c = \frac{\Delta H_{Fus}}{\Delta H_{Fus}^o} \tag{1}$$

The calculated thermal parameters from DSC are used to determine the probability density of crystalline melting as a function of temperature as given by $f(T)$ (Eq. (2)) where ΔH_m is the heat of fusion per unit mass for the perfect crystal, $P(T)$ is the DSC power output, ρ_c is the crystalline density, M is the sample mass, and α_m is the mass fraction crystallinity of the sample [13].

$$f(T)dT = \frac{1}{\alpha_m \Delta H_m} \frac{P(T)dT}{M\left(\frac{dT}{dt}\right)} \tag{2}$$

$$l = \frac{2\sigma_e 10^3}{\Delta H_m \rho_c \left(1 = \frac{T_m}{T_m^o}\right)} \tag{3}$$

$$g(l) = KP(T)(T_m^o - T)^2 nm^{-1} \tag{4}$$

$$K = \frac{\rho_c}{2\sigma_e T_m^o M \alpha_m 10^{19} \left(\frac{dT}{dt}\right)} \tag{5}$$

The constant parameters for polyethylene are T_m^o=418.7 K, ΔH_m=288 kJ/kg, σ_e=90 mJ/m^2, and ρ_c=967 kg/m^3 and the

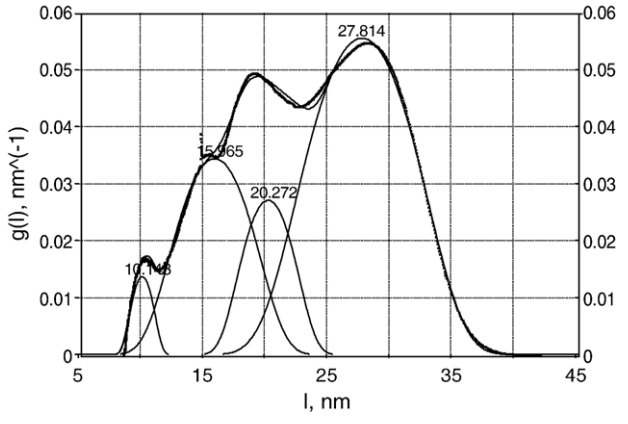

Fig. 3. Deconvolution of $g(l)$ distribution for UHMWPE sample exposed to low radiation dose.

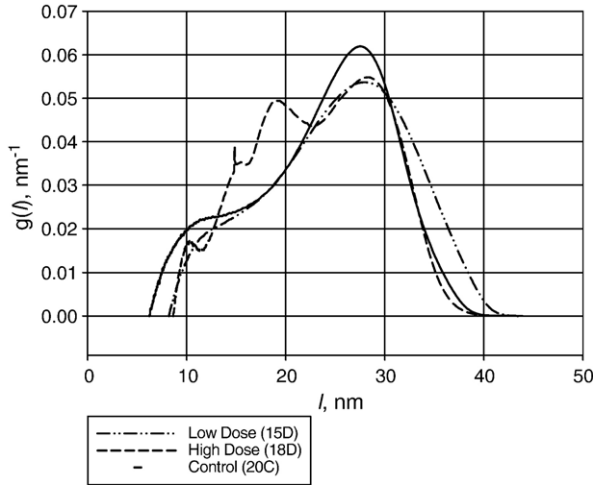

Fig. 5. Deconvolution of the $g(l)$ distribution for pristine UHMWPE (Control) sample.

Table 2
Peak melting temperature and crystallinity of pristine and irradiated UHMWPE

	Melting temperature				Crystallinity
	Peak 1	Peak 2	Peak 3	Peak 4	
Control		404.9±1.4	408.8±0.7	410.4±0.5	54.4±1.7
Low dose		401.8±2.7	409.5±0.5	410.6±0.4	57.6±2.9
High dose	390.2±1.8	399.1±0.9	404.0±0.5	410.2±0.8	61.8±5.8

sample dependent parameters are T_m in K, α_m, M in kg, dT/dt in K per second and $P(T)$ in mW [13]. An apparent crystal thickness distribution is calculated from transferring $f(T)$ into an equation dependent on l, the crystal thickness (Thompson equation, Eq. (3)) and the weight distribution function of thickness, $g(l)$ (Eqs. (4) and (5)). In these equations, σ_e is the basal surface energy, T_m^o is the melting temperature for an infinite crystal, and T_m is the melting temperature of the sample [13–15].

Deconvolution of the DSC thermograms and crystallite thickness distributions was performed using PeakFit® v.4.12. DSC thermograms were deconvoluted using extreme value 4 parameter fronted type peaks and the crystallite thickness distributions were deconvoluted using either error (amplitude) or beta (amplitude) type peaks.

3. Results and discussion

3.1. As Irradiated Ultra High Molecular Weight Polyethylene

3.1.1. Determination of Probability Functions

The DSC thermograms for the pristine and irradiated UHMWPE were converted into a probability distribution function on lamella thickness using Eqs. (2), (3), (4), and (5). The probability functions for the pristine and irradiated UHMWPE samples and their deconvoluted peaks are given in Figs. 2–4. Both the pristine and low radiation dose U7HMWPE exhibit a bimodal $g(l)$ distribution. The existence of two distinct populations of crystallite size is supported by earlier work from our laboratory [16] and Prenmath et al. [1]. The $g(l)$ distribution for the UHMWPE exposed to high proton radiation dose indicates the presence of at least four populations of crystallite size. The difference between the distribution functions is presented in the composite plot, Fig. 5.

3.1.2. Determination of the degree of crystallinity and melting temperature

The degree of crystallinity for the proton irradiated UHMWPE samples was determined from the ratio of the heat of fusion of the sample, ΔH_{FUS} and heat of fusion for a 100% crystalline polyethylene, ΔH^o_{FUS}, (Eq. (1)) [17]. A value of 288 J g^{-1} was used as the heat of fusion for a 100% crystalline polyethylene [18]. The degree of crystallinity as determined from DSC thermograms and the peak melting temperatures for the first run are summarized in Table 2. The degree of crystallinity increased slightly for the proton irradiated UHMWPE. Similarly, only a small variation is observed for the deconvoluted melting temperature of the irradiated samples. The lower melting temperature for peaks 1, 2, and 3 for the UHMWPE sample exposed to high proton radiation is a clear indication of the formation of smaller or less perfect crystallites due to possible changes in the length of crystallizable sequences. The increase in the degree of crystallinity of the irradiated samples can be attributed to crystallite formation as a result of the scission of tie chains during the exposure to proton radiation. A similar effect was observed for gamma irradiated UHMWPE [16].

3.1.3. Determination of crystallizable fractions

The crystallizable fractions of the pristine and irradiated UHMWPE samples were determined using Eq. (6), where "'x is the mole fraction of crystallizable units and ΔH_u is the molar heat of fusion of repeat units in the crystals [19].

$$\frac{1}{T_m^c} = \frac{1}{T_m^o} - \frac{R}{\Delta H_u} \ln x \tag{6}$$

The mole fraction of crystallizable units for pristine and irradiated UHMWPE samples are summarized in Table 3. These calculations were performed using the deconvoluted melting temperatures obtained from the DSC thermogram. It is important to note the similarity in the fractions obtained for the pristine and low dose samples. The similarity between the overall mole fractions of crystallizable units in the pristine and low dose samples indicates negligible crosslinking effects of the low proton radiation dose on UHMWPE. Samples exposed to high radiation dose exhibit an overall decrease in the mole fraction of the crystallizable units. This decrease can be attributed to the formation of more crosslink junctions, which contributes to a reduction of the crystallizable fraction.

3.1.4. Determination of the sequence length distribution

The presence of chain entanglements and crosslinks in irradiated UHMWPE permits the application of copolymer theory [20]. The rationale is based on the recognition that non-crystallizable units (chain entanglements and/or crosslinks) cannot be incorporated into the crystallite structure. Each crystallizable sequence is terminated by two non-crystallizable,

Table 3
Mole fractions of crystallizable units and sequence length in pristine and irradiated UHMWPE

	Crystallizable fraction				Sequence length (no. of repeat units)			
	Peak 1	Peak 2	Peak 3	Peak 4	Peak 1	Peak 2	Peak 3	Peak 4
Control		0.981±0.002	0.987±0.001	0.989±0.001		59.7±13.5		107.9±1.6
Low dose		0.977±0.004	0.988±0.001	0.989±0.001		55.5±3.6		108.7±4.1
High dose	0.960±0.003	0.973±0.001	0.980±0.001	0.989±0.001	37.5±3.4	58.3±6.5	73.3±9.2	110.1±0.9

Table 4
Crystal thickness

	1st moment	2nd moment	Peak 1	Peak 2	Peak 3	Peak 4
Control	16.8±2.3	19.8±2.1		15.1±3.4		27.4±4.0
Low dose	17.4±2.4	21.0±1.7		13.1±1.4		27.6±1.0
High dose	16.5±2.7	20.8±1.9	9.5±0.9	14.8±1.6	18.6±2.3	28.0±0.2

units and thus defines the time scale of crystallization, size of crystal and level of crystallinity. The sequence length was calculated for each crystal present in the thickness distribution and summarized in Table 3. Both the pristine and low dose samples exhibit a similar bimodal sequence length distribution. The samples exposed to high proton doses have four distinct sequence distributions. One of the additional sequence distributions is intermediate between the two observed for the low dose and pristine samples while the other is much shorter. The existence of four distinct sequence lengths in the samples exposed to high proton radiation dose is indicative of the random nature of crosslinking of molecular chain associated with the irradiation process and leads to formation of at least four distinct crystallite size populations. The ability of cross linked polymers to crystallize depends on the crystallizable sequence length distribution because it ultimately defines the time scale of the crystallization, size of crystals and level of crystallinity. At a given temperature a sequence length must exceed a critical value prior to participation in the nucleation process [21].

3.1.5. Crystallite thickness

The average thicknesses of crystals formed during the proton irradiation of UHMWPE samples are compared to the pristine (control) sample in Table 4. The samples that were exposed to low doses of proton radiation exhibit similar thickness to the control sample. The high dose samples show two new crystals with a low and intermediate thickness of 9.54 and 18.63 nm, respectively. The two new peaks are directly related to changes in the sequence length distribution resulting from the increase in the concentration of non-crystallizable units in the molecular chain.

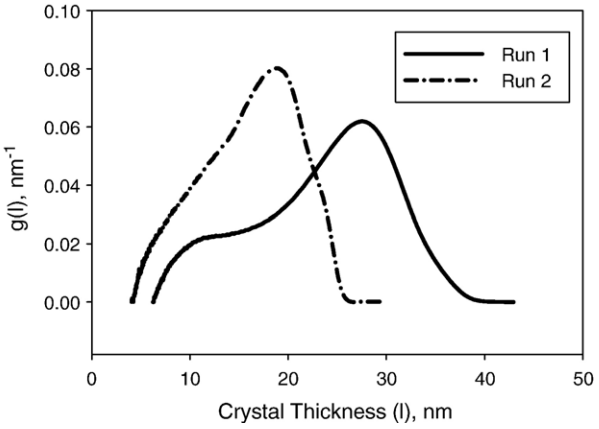

Fig. 6. Composite crystal thickness plot.

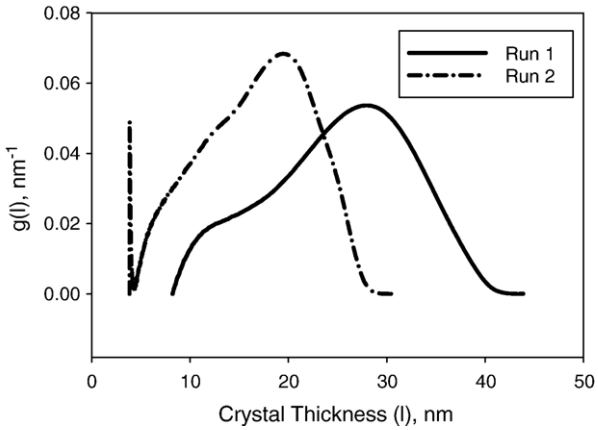

Fig. 7. Comparison between first and second DSC run for control samples.

3.2. Analysis of heat treated irradiated UHMWPE

In addition to impact from high-energy particles, objects placed in the space environment may be subjected to variations in temperature. The irradiated UHMWPE samples were subjected to a second heating to simulate thermal cycling which shielding materials could be exposed to in space.

3.2.1. Determination of the probability functions

The DSC thermograms for the second heating cycle were converted into a function on lamella thickness as described earlier in this work. The probability functions for the pristine and irradiated UHMWPE samples are given in Figs. 6–8. A comparison of the distribution functions for the initial heating (first run) and heat treatment (second run) of the pristine and irradiated UHMWPE samples is also presented in Figs. 6–8. In general, the $g(l)$ distribution for irradiated UHMWPE samples indicates a shift to lower crystallite size. The results from the deconvolution will be presented in the subsequent sections.

3.2.2. Determination of the degree of crystallinity and melting temperature

The degree of crystallinity for the proton-irradiated heat-treated UHMWPE samples was determined by the procedure

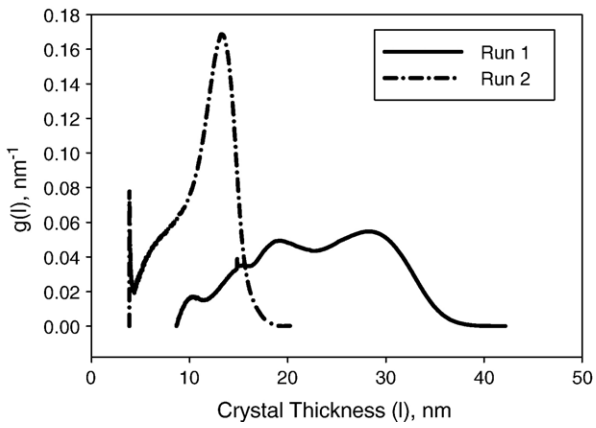

Fig. 8. Comparison between first and second DSC run for low dose samples.

Table 5
Degree of crystallinity and melting temperatures for heat treated irradiated UHMWPE

	Melting temperature			Crystallinity
	Peak 1	Peak 2	Peak 3	
Control	402.3±1.8	405.9±1.1	407.5±0.8	58.5±3.5
Low dose	395.7±3.6	405.2±0.5	407.5±0.4	60.3±2.2
High dose	390.7±5.5	399.2±0.4		55.3±5.4

described earlier in this work. The degrees of crystallinity, as determined from DSC thermograms and peak melting temperatures for the second run, are summarized in Table 5. The pristine and low dose samples showed slight increases in the degree of crystallinity when compared to first heating. The degree of crystallinity appeared to decrease for the high dose proton irradiated UHMWPE. The melting temperatures for the pristine and heat treated irradiated UHMWPE samples decreased by a couple of degrees possibly due to changes in the crystallization condition. The high-temperature melting peak previously observed (first run) for the samples irradiated at high proton doses is missing. The absence of the higher melting peak is an indication of the formation of smaller or less perfect crystallite due to possible changes in the length of crystallizable sequences.

3.2.3. Sequence length distribution and crystallizable fraction

The heat treatment of irradiated UHMWPE leads to noticeable changes in the sequence length distribution, as seen in Table 6. Since there is a correspondence between sequence length distribution and crystallite size distribution, changes in the sequence length distribution should be reflected in the crystallite size. The major difference is observed for samples subjected to high proton radiation dose where the peak sequence length decreases from 96 to 53 repeat units and actual length decreased for all peaks. The smaller sequence length distribution for the high dose should translate to smaller crystallites. The disappearance of previously observed crystals is due in part to formation of segments smaller than the critical size segment length required to participate in the nucleation process.

3.2.4. Crystallite thickness

The re-heating of the irradiated UHMWPE samples leads to changes in the size of the crystallites. The control samples previously included crystallites having two distinct sizes, 15.2 and 27.4 nm. After the heat treatment, the number of crystallite sizes present increased to three, 13.1, 19.2, 24 nm.

Table 7
Crystal thickness distribution in pristine and heat treated irradiated UHMWPE

	1st moment	2nd moment	Peak 1	Peak 2	Peak 3
Control	12.0±0.9	14.6±0.6	13.1±1.7	19.2±0.1	23.9±0.7
Low dose	11.6±1.1	14.1±0.6	11.4±2.7	19.0±1.5	23.4±1.2
High dose	9.5±0.6	10.6±0.4	8.4±1.4	13.3±1.1	

The morphology of samples exposed to low proton radiation dose also includes three different crystallite sizes (11.5, 19.1 and 23.4 nm) with fairly close values to those observed for the pristine (control) samples. The UHMWPE samples exposed to high proton radiation dose exhibited the largest changes in their morphology with the number of crystallite sizes decreasing from four (9.5, 14.8, 18.6 and 28 nm) to two, much smaller crystallites (8.4 and 13.3 nm). This signifies the existence of a highly cross-linked system with relatively shorter crystallizable sequence lengths (30 and 53 repeat units). The similarity in the thermal behavior of the control and low dose samples supports the notion that low doses of proton irradiation produce very little change in the morphology of UHMWPE (Table 7).

4. Conclusions

Proton irradiation of UHMWPE produces morphological changes in the mole fraction of crystallizable units, sequence length distribution, and crystallite thickness and distribution. The type of morphological changes is dependent on the irradiation dose and thermal cycle. The low dose proton irradiation produces only slight changes in the morphology of UHMWPE. More pronounced morphological changes are observed for the higher dose proton irradiation. Low dose proton irradiation in the presence of oxygen does lead to the formation of very low-levels of intermolecular crosslinks in UHMWPE, as seen by the negligible difference in the sequence length in both the as-irradiated and heat treated samples. High doses of proton irradiation produce significant levels of intermolecular crosslinks in UHMWPE, which can be seen from the formation of a crystallite thickness distribution with four modes and the reduction of sequence length in the heat treated form from 48, 76, and 97 repeat units in the control to 30 and 53 repeat units.

Acknowledgements

The researchers would like to thank Tim Stephens for assistance in collecting DSC data.

Table 6
Sequence length and crystallizable fraction distribution in pristine and heat treated irradiated UHMWPE

	Crystallizable fraction			Sequence length (no. of repeat units)		
	Peak 1	Peak 2	Peak 3	Peak 1	Peak 2	Peak 3
Control	0.978±0.003	0.983±0.002	0.985±0.001	47.6±9.6	76.3±1.3	96.7±5.4
Low dose	0.968±0.005	0.982±0.001	0.985±0.001	45.1±10.6	75.0±6.1	92.0±4.8
High dose	0.961±0.008	0.973±0.001		30.5±4.1	52.7±0.5	

References

[1] V. Premnath, A. Bellare, E.W. Merrill, M. Jasty, W.H. Harris, Polymer 40 (1999) 2215.
[2] G. Lewis, Biomaterials 22 (2001) 371.
[3] R.S. Benson, C.P. Stephens, Ma. E. Martinez-Pardo, J. Appl. Med. Polym. 6 (2) (2002).
[4] O. Tretinnikov, S. Ogata, Y. Ikada, Polymer 39 (24) (1998) 6115.
[5] L. Guadagno, C. Naddeo, V. Vittoria, G. Camino, C. Cagnani, Polym. Degrad. Stab. 72 (2001) 175.
[6] B. Hollis, Analysis of the Wear Behavior of VUV Radiated Ultrahigh Molecular Weight Polyethylene, The University of Tennessee, Knoxville, TN, 1999.
[7] M. Morrison, Effect of Crosslinking on the Tribological Properties of Ultra-high Molecular Weight Polyethylene, in Materials Science and Engineering, The University of Tennessee, Knoxville, TN, 2002.
[8] J.F. Wilson, J.R. Liu, F. Romero-Borja, W.K. Chu, Proton modification of ultra high molecular weight polyethylene to promote crosslinking for enhanced chemical and physical properties. Mater. Res. Soc. Symp. Proc., 1996. 396 (Ion-Solid Interactions for Materials Modification and Processing), p. 311–316.
[9] J.F. Wilson, J.R. Liu, F. Romero-Borja, W.-K. Chu, J. Mater. Res. 14 (11) (1999) 4431.
[10] T. Sasuga, H. Kudoh, T. Seguchi, PSF PES. Polym. 40 (18) (1999) 5095.
[11] M.E. Martinez-Pardo, J. Cardoso, H. Vazquez, M. Aguilar, Nucl. Instrum. Methods Phys. Res., B Beam Interact. Mater. Atoms 140 (3,4) (1998) 325.
[12] C.P. Stephens, Society of Plastics Engineers Annual Technical Conference, 2003, Nashville, TN, 2003.
[13] B. Crist, F.M. Mirabella, J. Polym. Sci., Part B, Polym. Phys. 37 (1999) 3131.
[14] A. Valles-Llunch, L. Contat-Rodrigo, A. Ribes-Greus, J. Appl. Polym. Sci. 89 (2003) 3260.
[15] J.T.E. Cook, P.G. Klein, I.M. Ward, A.A. Brian, D.F. Farrar, J. Rose, GPC DSC. Polym. 41 (2000) 8615.
[16] C. Stephens, R. Benson, M. Martinez-Pardo, E. Barker, J. Walker, T. Stephens, Nucl. Instrum. Methods Phys. Res., B Beam Interact. Mater. Atoms 236 (2005) 540.
[17] H.F. Ferguson, D.J. Frurip, A.J. Pastor, L.M. Peerey, L.F. Whiting, Thermochim. Acta 363 (2000).
[18] A. Shinde, R. Salovey, J. Polym. Sci., Polym. Phys. Ed. 23 (1985) 1681.
[19] P. Flory, J. Trans. Faraday Soc. 51 (1955) 848.
[20] H. Kilian, K. Unseld, E. Jaeger, J. Muller, B. Jungnnickel, Colloid Polym. Sci. 263 (1985) 607.
[21] R. Alamo, L. Mandelkern, Crystallization kinetics of random ethylene copolymers, Macromology 24 (1991) 6480.